ANNALS OF GEOPHYSICS, VOL. 48, N. 3, June 2005

A dynamic system to forecast ionospheric storm disturbances based on solar wind conditions

Ioanna Tsagouri ([1]), **Anna Belehaki** ([1]) **and Ljiljana R. Cander** ([2])
([1]) *Ionospheric Group, Institute for Space Applications and Remote Sensing, National Observatory of Athens, Palaia Penteli, Greece*
([2]) *Rutherford Appleton Laboratory, Chilton, Didcot, Oxon, U.K.*

Abstract
For the reliable performance of technologically advanced radio communications systems under geomagnetically disturbed conditions, the forecast and modelling of the ionospheric response during storms is a high priority. The ionospheric storm forecasting models that are currently in operation have shown a high degree of reliability during quiet conditions, but they have proved inadequate during storm events. To improve their prediction accuracy, we have to take advantage of the deeper understanding in ionospheric storm dynamics that is currently available, indicating a correlation between the Interplanetary Magnetic Field (IMF) disturbances and the qualitative signature of ionospheric storm disturbances at middle latitude stations. In this paper we analyse observations of the *foF*2 critical frequency parameter from one mid-latitude European ionospheric station (Chilton) in conjunction with observations of IMF parameters (total magnitude, *Bt* and *Bz*-IMF component) from the ACE spacecraft mission for eight storm events. The determination of the time delay in the ionospheric response to the interplanetary medium disturbances leads to significant results concerning the forecast of the ionospheric storms onset and their development during the first 24 h. In this way the real-time ACE observations of the solar wind parameters may be used in the development of a real-time dynamic ionospheric storm model with adequate accuracy.

Key words *inospheric forecasting – ionospheric modelling – ionospheric storms*

1. Introduction

Access to real-time information on ionospheric conditions over a certain area (*e.g.*, Europe), as a requirement for high frequency communication, satellite-to-ground links, and solar-terrestrial research, requires: a) a network of vertical ionosondes covering as large an area as possible with real-time data access (Hanbaba, 1999); b) short-term forecasting algorithms to be developed for *foF*2, M(3000)*F*2, and TEC to predict their values up to 24 h ahead (Kutiev *et al.*, 1999; Hochegger *et al.*, 2000); c) a mapping algorithm for interpolation between the stations in the network to be implemented by using one of the available mapping procedure (Samardjiev *et al.*, 1993); d) validation of the mapping and forecasting algorithms. As a response to these needs, an operational Short-Term Ionospheric Forecasting (STIF) tool for the European region based on continuous monitoring of the ionosphere has been developed and is available on the World Wide Web for interactive use (http://ionosphere.rcru.rl.ac.uk) (Cander, 2003, and references therein). It provides forecasting maps for up to 24 h ahead and archive measurement maps of the critical frequency *foF*2 of the ionospheric *F*2-layer, the Maximum Usable Frequency for a

Mailing address: Dr. Ioanna Tsagouri, Ionospheric Group, Institute for Space Applications and Remote Sensing, National Observatory of Athens, Metaxa and Vas. Pavlou str., 15236 Palaia Penteli, Greece; e-mail: tsagouri@space.noa.gr

3000 km range MUF(3000)*F*2, NeQuick modelled vertical Total Electron Content (TEC), and Frequency of Optimum Traffic (FOT) for the area of interest at each UT hour. A similar technique can be applied in any other areas, like U.S.A., Australia, China, where enough data are available in timely form.

Accuracy of forecast of *foF*2, MUF(3000)*F*2 and TEC has been studied through several statistical comparisons between measured and forecast values of *foF*2 and MUF(3000)*F*2 (Cander *et al*., 2003). The forecast values selected were those deduced for one day ahead of the measured values. The principal results concern: 1) comparisons at each UT hour during 10 geomagnetically quiet days of each month in two years of maximum solar activity in the current solar cycle 2000 and 2001; and 2) comparisons at each UT hour during 5 geomagnetically disturbed days of each month in the same years. These gave the Root Mean Square Error (RMSE) of approximately 0.76 MHz for *foF*2 and 2.51 MHz for MUF(3000)*F*2 respectively and Normalised RMSE (NRMSE) of 0.17 for both in the case of the geomagnetically quiet ionosphere. Figure 1 shows an example of the typical STIF *foF*2 and MUF(3000)*F*2 results and measurements during seven quiet days of December 2001.

Global statistical comparisons for the 5 most disturbed days in 2000 and 2001 gave RMSE for *foF*2 and MUF(3000)*F*2 of 1.48 MHz and 4.38 MHz, respectively and NRMSE=0.67 for both. It should be noted that individual hourly RMSE in MUF(3000)*F*2 are generally about three times those of *foF*2. This is to be expected as M(3000)*F*2 propagation factors are typically about 3 though additional errors can be introduced by the measurements of the M(3000)*F*2 factor. Figure 2 shows an example of the typical STIF *foF*2 and MUF(3000)*F*2 results and measurements during seven extremely disturbed days of March and April 2001. These results clearly suggest that the STIF tool provides a very reliable forecasting technique in relatively quiet geomagnetic conditions. Although these conditions prevail in the normal Earth's ionosphere, the conditions during the geomagnetic storms are of high importance for current and future radio communications services as well as space weather operational requirements and scientific studies, and under such conditions STIF has been proved inadequate.

STIF weakness concerns the forecast of the ionospheric storms onset and their development during the first 24 h. To improve its prediction accuracy we have to include recent scientific and technological advances. Recent studies on ionospheric dynamics during geomagnetic storm events in the light of the global solar wind-magnetosphere-ionosphere interaction suggest that the ionospheric response depends on the solar wind conditions leading to geomagnetic storms and on the intensity of the storm. For example, Belehaki and Tsagouri (2002), in an investigation of the nighttime ionospheric response at middle latitudes, related the recording of positive storm effects from ground ionosondes at night with the type of the storm. Geomagnetic storms with initial phases, followed by short in duration but very fast evolving main phases, produce nighttime ionization depletion as a global effect at middle latitudes, independent of the storm intensity. During gradual driven storms, positive storm effects are frequently observed at middle to low latitudes. Given that geomagnetic storms are gradually evolving, the observation of positive effects at night depends also on the storm intensity and the latitude of the observation point. The critical point in the explanation of the two different types of ionospheric response to different types of storms is the expansion of the neutral composition zone (Belehaki and Tsagouri, 2002). The sudden orientation of the IMF to a very large southward field severely disturbs the magnetosphere-ionosphere system and changes the effective input energy to the auroral ionosphere, causing the very fast expansion of the deep negative phase equatorward. In contrast, during gradually evolving storms the neutral composition disturbance zone remains restricted to high latitudes, and the middle to low latitudes ionosphere is affected by other competing mechanisms. In the light of these findings, one could argue that the forecast of the type of the storm and of storm intensity could lead to a prediction of the ionospheric response at middle latitudes. The crucial feature that determines the storm type is the arrival of a shock wave in the earth vicinity, which can be identified by the rate of change of *Bz*-IMF (*dBz*/*dt*), which is also indicative of the rate of

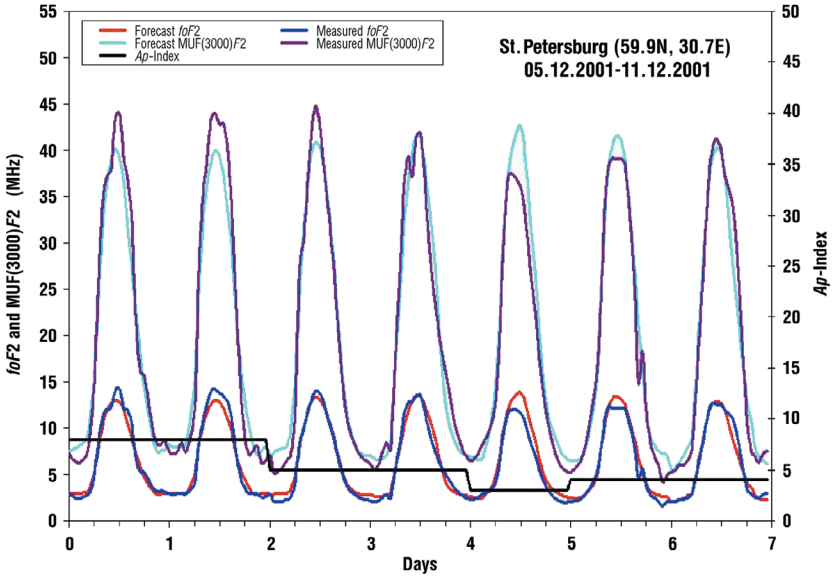

Fig. 1. Comparison between measured and STIF forecast *foF*2 (blue and red line, respectively) and MUF(3000)*F*2 (dark magenta and cyan line, respectively) values at St. Petersburg ionosonde station with *Ap* values (black line) as an indicator of the low geomagnetic activity.

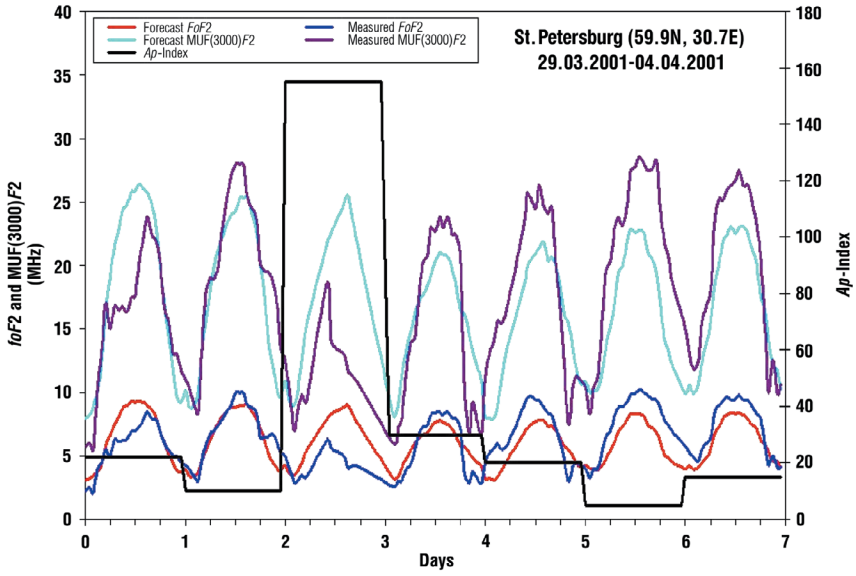

Fig. 2. Comparison between measured and STIF forecast *foF*2 (blue and red line, respectively) and MUF(3000)*F*2 (dark magenta and cyan line, respectively) values at St. Petersburg ionosonde station with *Ap* values (black lines) as an indicator of the high geomagnetic activity.

the solar wind energy entering the magnetosphere-ionosphere system.

The NASA Advanced Composition Explorer (ACE) spacecraft at the vantage *L*1 point performs measurements over a wide range of energies and nuclear masses, under all solar wind flow conditions, and during both large and small particle events including solar flares. The data are fundamental to enabling the formulation of highly accurate forecasting techniques and the subsequent issue of alerts and warnings of incoming major geomagnetic disturbances and their possible effects on the structures in ionospheric layers variations (Kappenman, 1998). The time delay for the solar wind to travel from the *L*1 point where ACE is to the Earth is about one hour, giving forecaster the advanced knowledge of the storm type one hour before its consequences are detectable in the Earth's environment. Therefore, the data from ACE could be a useful tool in real time ionospheric space weather forecasting.

This contribution is an investigation of the ionospheric response to interplanetary magnetic field disturbances with the primary goal of developing the understanding and the means to forecast how the ionospheric *F*2-layer will respond to abruptly and dramatically changing solar and geomagnetic conditions. It is an attempt to use the Real-Time Solar Wind (RTSW) data from the ACE spacecraft mission to derive criteria for issuing alerts for forthcoming major geomagnetic storms, as one of the dominant space weather events, and their effects on the ionospheric critical frequency *foF*2 in the first 24 h.

2. The effect of solar wind conditions in ionospheric storm development

One of the most popular and complete descriptions of the ionospheric storm-induced effects is the Prölss phenomenological model (Prölss, 1993), which was extended by Fuller-Rowell *et al*. (1994, 1996). This model captures most of the basic aspects of ionospheric storms, such as the long-lived negative storm effects and daytime positive effects. Negative storm effects are attributed to the formation and evolution of the neutral composition bulge. The magnitude and the distribution of the negative ionospheric phase depend on the magnitude and the position of the neutral composition bulge. Since the expansion of the neutral composition zone has been related to the solar wind conditions under which the global solar wind-magnetosphere-ionosphere coupling occurs (Belehaki and Tsagouri, 2002), it is reasonable to investigate, as a next step, the temporal correlation between the occurrence of IMF disturbances and the recording of negative storm phases at middle latitudes.

For this purpose we analyse hourly observations of the *foF*2 critical frequency parameter from Chilton station (http://www.wdc.rl.ac.uk) in conjunction with hourly observations of interplanetary magnetic field parameters (total magnitude and *Bz*-IMF component) from the ACE

Table I. List of the storms used in this study.

Start and main days	*Dst* (nT)	Chosen quiet days	Onset sector (UT)	Onset of IMF disturbances (UT)
21-22 October 1999	–237	07 October 1999	Midnight	23:00
06-07 April 2000	–288	22 April 2000	Noon	14:00
15-16 July 2000	–301	08 July 2000	Noon	13:00
11-12 August 2000	–235	19 August 2000	Midnight	22:00
30-31 March 2001	–358	11 March 2000	Midnight	23:00
11-12 April 2001	–256	26 April 2001	Noon	12:00
05-06 November 2001	–277	12 November 2001	Midnight	23:00
07-08 September 2002	–170	01 September 2001	Noon	12:00

spacecraft mission (http://cdaweb.gsfc.nasa.gov/cdaweb/istp_public) and hourly records of the *Dst*-index (http://swdcdb.kugi.kyoto-u.ac.jp/wdc) for eight intense storm events. Table I presents a list of the storm events used in this study, together with the minimum *Dst* values. The ionospheric response was considered in terms of the ratio $foF2_{observed}/foF2_{quiet}$, where $foF2_{quiet}$ represents the diurnal quiet time behaviour for Chilton. The latter was formed by the records of the chosen quiet day for each month. The selection of the quietest day of the month was based on the inspection of the *Dst* values and it is also given in table I. In an attempt to classify the storm events, we note the onset sector for each event in the fourth column of table I, referring to the sector where Chilton was when the onset of the IMF disturbances occurred. The onset of the IMF disturbances was determined as the time of sudden increase in the solar wind magnetic field *Bt*, which denotes an abrupt increase in the solar wind energy that enters the Earth's magnetos-

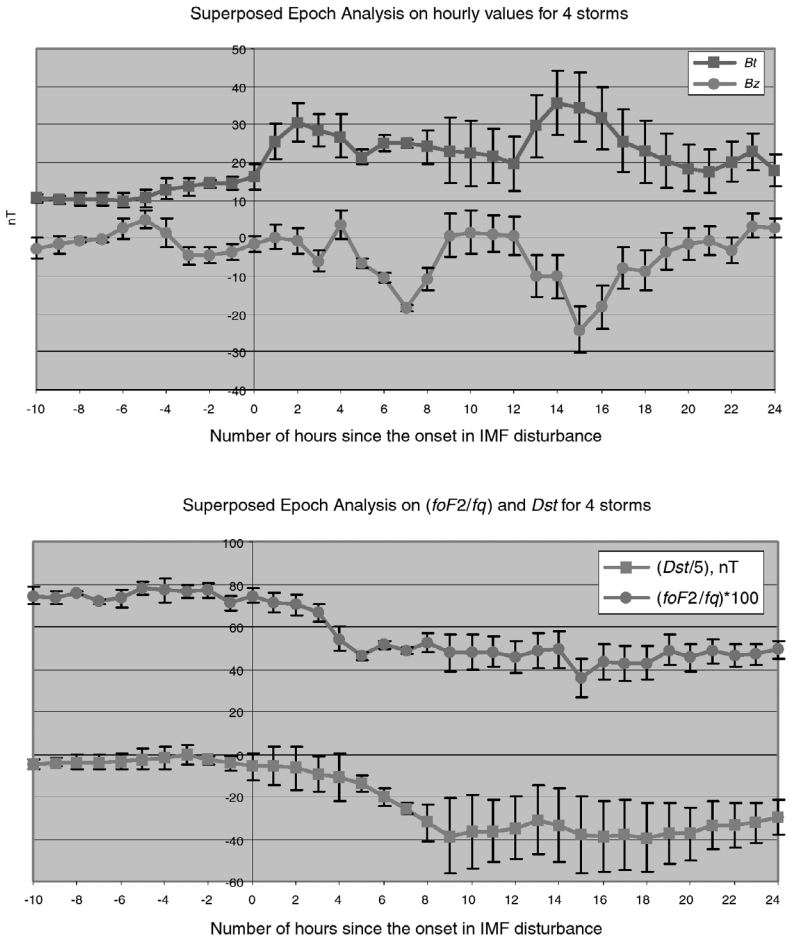

Fig. 3. The results of the superposed epoch analysis on *Bt*, *Bz*, *foF*2/*fq* and *Dst* for the four storm events with near midnight onset. The vertical bars represent the standard deviation computed from the whole stack of superposed traces.

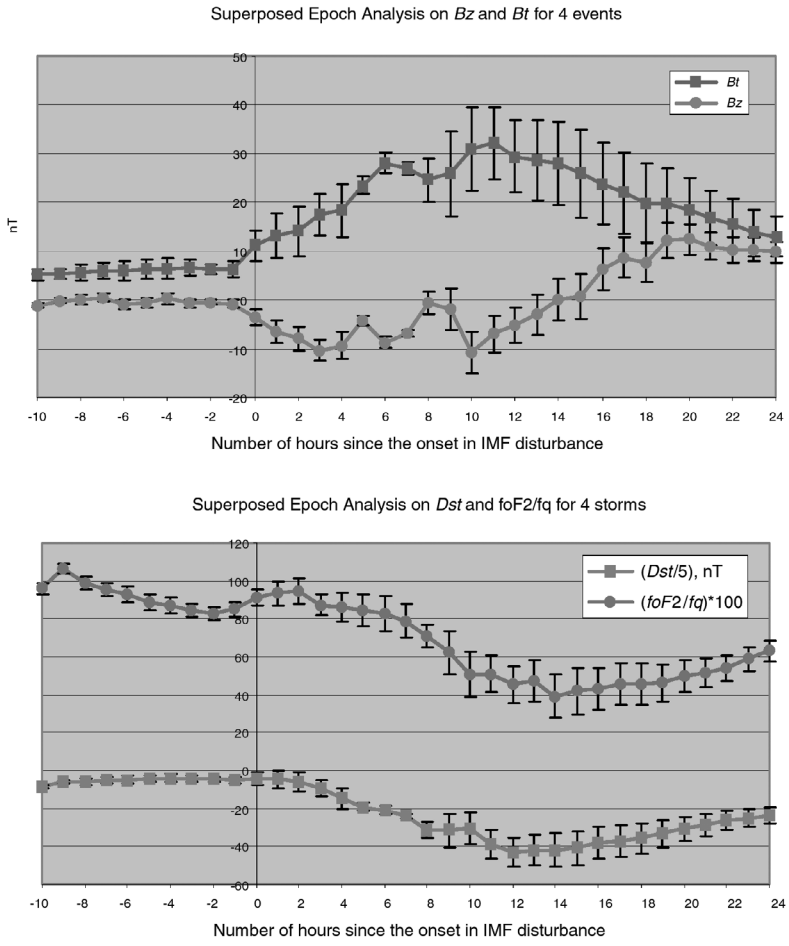

Fig. 4. The results of the superposed epoch analysis on *Bt*, *Bz*, *foF*2/*fq* and *Dst* for the four storm events with onset near noon. The vertical bars represent the standard deviation computed from the whole stack of superposed traces.

phere. It is obvious that the eight storm events may be separated into two groups: the first includes the 4 storms with a near midnight onset, while the second includes the 4 storms with onset near noon. Then, a superposed epoch analysis was applied on the *Bt*, *Bz*, *foF*2/*fq*, and *Dst* for both groups in order to obtain an overall perspective of the observations time sequence. The results are given in figs. 3 and 4, respectively.

Figure 3 shows the results of the superposed epoch analysis on *Bt*, *Bz*, *foF*2/*fq* and *Dst* for the four storm events with near midnight onset. A rapid increase in *Bt* was followed by southward turning of the *Bz*-IMF component, indicating that the solar wind energy entering in the magnetosphere-ionosphere system increases rapidly. The *Bz*-IMF southward turning triggered the onset of the geomagnetic storm, as this was recorded by the *Dst*-index with no significant time delay. At the same time the middle latitude ionosphere responded almost immediately to drastic changes in IMF parameters with significant negative storm effects and a deep negative phase recorded in Chilton.

Figure 4 shows the results of the superposed epoch analysis on *Bt*, *Bz*, *foF*2/*fq* and *Dst* for the four storm events with onset near noon. The rapid increase in *Bt* was recorded simultaneously with the southward turning of *Bz*-IMF component that triggered the onset of the geomagnetic storm and consequently the observed decrease of the *Dst*-index with a time delay of 2 h. Significant negative storm effects in the middle latitude ionosphere were recorded 6 h later and when the Chilton station had been rotated in the evening sector. This latter observation is also consistent with Prölss's phenomenological scenario.

Two interesting features are extracted from the above preliminary analysis: in the first case when the IMF disturbances occurred near midnight, the evolution of *Dst*-index and the ionospheric response in Chilton occurred simultaneously. This means that the *Dst*-index cannot be used as a prediction tool for ionospheric forecasting. On the other hand, the time delay between the IMF disturbances and the ionospheric response seems to depend on the onset time sector. But even near midnight when the ionospheric response is expected to be direct we can count on the quite safe time delay of one hour required for the solar wind disturbance, once it is detected by ACE, to reach the Earth. Of course, statistical studies based on a large sample of events are needed to establish these results but in general, they reveal a unique opportunity to predict the *F*2-layer response to geomagnetic storm by using the ACE data in near real time mode.

To work further on the idea of developing a real time dynamic system to forecast ionospheric storm effects in middle latitudes in operational form, we calculated the *Bz* rate of change, *dBz*mod (*dBz*mod = 100**dBz*/*dt*) over the preceding 20 min time interval and the percentage deviation of hourly *foF*2 from median values, *dfoF*2 (%), for Chilton for all the events listed in table I. Here we present an example of the impulse type of geomagnetic storm on 30 March 2001 with initial compressive phase and very fast evolving main phase, triggered by an interplanetary shock wave in fig. 5.

Figure 5 shows the *dfoF*2 (%) immediate response to the sudden and significant changes of

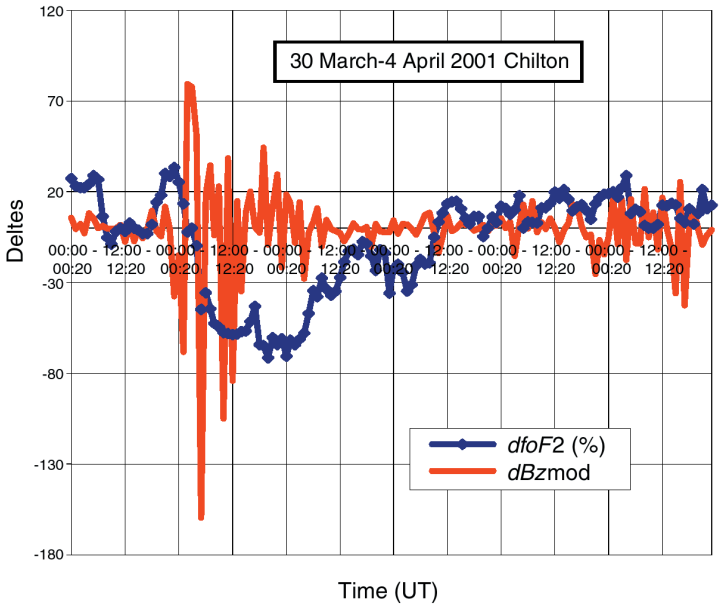

Fig. 5. *Bz* rate of change in 20 min interval with corresponding *foF*2 response for March 30, 2001 storm as seen at Chilton ionosonde station (51.5°N, –1.3°E).

the *Bz* expressed by *dBz*mod. Minutes after *dBz*-mod changes from +70 to −100, the *dfoF*2 (%) revealed a huge negative response of more than 50% followed by a decrease of up to −70% during the main phase of the storm. The negative storm effect over Chilton was dominant for more than 36 h. This example illustrates the knowledge required to the development of a successful real-time dynamic ionospheric storm forecasting algorithm. In that context a time delay between measurements can have a significant role and will be the subject of further studies.

3. Discussion

The ionospheric critical frequency of the *F*2-layer is highly variable on time-scales ranging from decades to seconds with the occurrence of ionospheric disturbances associated with geomagnetic storms. Many attempts have been made recently in Europe to study the space environmental disturbances frequently referred to as space weather (Cander, 2003). In these studies the focus is on forecasting the geomagnetic storm effect on the main ionospheric parameters to enable extreme conditions to be quantified so that particularly for telecommunications planning likely variability bounds can be defined. In general, forecasts are made mostly on the basis of persistence and recurrence that are not always strong. The current existing 24 h forecasting service (http://ionosphere.rcru.rl.ac.uk) relies heavily on an extrapolation of past and prevailing ionospheric conditions. In practice this requires an automation of the data collection and processing and on-line forecasting message distribution. There has been ample evidence from different national as well as international space weather research projects that true forecasts of ionospheric disturbances are needed with lead times of up to 24 h of the present. Very recently sufficient real-time data on interplanetary conditions (*e.g.*, solar-wind parameters) have been obtained to do this effectively (Kamide, 2000). However, *F*-region storm morphology has a complex spatial and temporal structure that requires continuous monitoring with high time resolution. In this paper we examined the solar-terrestrial conditions and ionospheric *F*2-layer responses associated with eight geomagnetic storms to illustrate what knowledge needs to be included in a successful real-time dynamic ionospheric storm forecasting algorithm. Such forecasting requires automatic daily retrieval of RTSW data from the ACE spacecraft mission at <http://sec.noaa.gov/Data> and the ionospheric characteristics from ionospheric stations operating in real-time in Europe from WDC-C1 at RAL (http://www.wdc.rl.ac.uk/cgi-bin/digisondes/ cost_database.pl). Currently an automated real-time dynamic system for monitoring ionospheric propagation conditions over Europe is operational at RAL (http://ionosphere.rcru.rl.ac.uk) in collaboration with National Observatory of Athens (Cander *et al*., 2004).

Acknowledgements

This work is part of the European Action COST271 and it was realised during a COST271 short-term mission of one of the authors I.T. in Rutherford Appleton Laboratory in the U.K.

REFERENCES

Belehaki, A. and I. Tsagouri (2002): On the occurrence of storm induced nighttime ionisation enhancements at ionospheric middle latitudes, *J. Geophys. Res*., **107** (8), 23,1-23,19.

Cander, Lj.R. (2003): Toward forecasting and mapping ionospheric space weather under the COST actions, *Adv. Space Res*., **31** (4), 957-964.

Cander, Lj.R, R. Bamford and J.G. Hickford (2003): Nowcasting and forecasting the *foF*2, MUF(3000)*F*2 and TEC based on empirical models and real-time data, *IEE Conf. Proc*., **491** (1), 139-142.

Cander, Lj.R, J.G. Hickford, I. Tsagouri and A. Belehaki (2004): Real-time dynamic system for monitoring ionospheric propagation conditions over Europe, *Electron. Lett*., **40** (4), 224-226.

Fuller-Rowell, T.J., M.V. Codrescu, R.J. Moffett and S. Quegan (1994): Response of the thermosphere and ionosphere to geomagnetic storms, *J. Geophys. Res*., **99**, 3893-3914.

Fuller-Rowell, T.J., M.V. Codrescu, H. Rishbeth, R.J. Moffett and S. Quegan (1996): On the seasonal response of the thermosphere and ionosphere to geomagnetic storms, *J. Geophys. Res*., **101**, 2343-2353.

Hanbaba, R. (1999): Improved quality of service in ionospheric telecommunication systems planning and operation, in *COST Action 251 Final Report*, Space Research Centre, Warsaw, 102-103.

Hochegger, G., B. Nava, S.M. Radicella and R. Leitinger

(2000): A family of ionospheric models for different uses, *Phys. Chem. Earth (C)*, **25**, 307-310.

KAMIDE, Y. (2000): From discovery to prediction of magnetospheric processes, *J. Atmos. Sol.-Terr. Phys.,* **62**, 1659-1668.

KAPPENMAN, J.G. (1998): Geomagnetic storm forecasting mitigates power system impacts, *IEEE Power Eng. Rev.*, **18** (11) (available on line at: http://www.spectrum.ieee.org/pubs/mags/9902/kapp.html).

KUTIEV, I., P. MUHTAROV, LJ.R. CANDER and M. LEVY (1999): Short-term prediction of ionospheric parameters based on autocorrelation analysis, *Ann. Geofis.*, **42** (1), 121-127.

PRÖLSS, G.W. (1993): On explaining the local time variation of ionospheric storm effects, *Ann. Geophysicae,* **11**, 1-9.

SAMARDJIEV, T., P.A. BRADLEY, LJ.R. CANDER and M.I. DICK (1993): Ionospheric mapping by computer contouring techniques, *Electron. Lett.*, **29** (20), 1974-1975.